Thin Solid Films 666 (2018) 15–19

Contents lists available at ScienceDirect

Thin Solid Films

journal homepage: www.elsevier.com/locate/tsf

Study of $Cu_2CdGeSe_4$ monograin powders synthesized by molten salt method for photovoltaic applications

M. Kauk-Kuusik[a,*], X. Li[a], M. Pilvet[a], K. Timmo[a], M. Grossberg[a], T. Raadik[a], M. Danilson[a], V. Mikli[a], M. Altosaar[a], J. Krustok[a,b], J. Raudoja[a]

[a] Department of Materials and Environmental Technology, Tallinn University of Technology, Ehitajate tee 5, 19086 Tallinn, Estonia
[b] Division of Physics, Tallinn University of Technology, Ehitajate tee 5, 19086 Tallinn, Estonia

ARTICLE INFO

Keywords:
Molten salt synthesis-growth
Crystal structure
Solar cells
Copper cadmium germanium selenide

ABSTRACT

$Cu_2CdGeSe_4$ monograin powders were synthesized by molten salt method for photovoltaic applications. The effects of salt material (CdI_2 and KI), synthesis temperature and time on the structural, morphological, compositional and optoelectronic properties were investigated. Phase analysis by Raman spectroscopy and X-ray diffraction methods showed that the $Cu_2CdGeSe_4$ powder crystals synthesized at 500 °C had tetragonal structure and those synthesized at 600 °C and 700 °C had orthorhombic structure. The band gap values determined from external quantum efficiency measurements were 1.27 eV for orthorhombic $Cu_2CdGeSe_4$ and 1.14 eV for tetragonal $Cu_2CdGeSe_4$ powder crystals. The monograin layer solar cell on the base of orthorhombic $Cu_2CdGeSe_4$ powder showed the best conversion efficiency of 4.21% (active area), with an open-circuit voltage of 0.46 V, a short-circuit current density of 23.3 mA/cm^2 and fill factor of 39%.

1. Introduction

There is a large group of ternary and quaternary copper chalcogenide compounds that have attracted considerable attention due to their suitable properties for thin film solar cell absorbers. Among them $Cu(In,Ga)Se_2$ (CIGSe) based thin film solar cells have been studied for several decades and resulted in power conversion efficiency (PCE) of 22.9% [1]. Another semiconductor material which responds to the requests of using only low-cost, non-toxic and earth-abundant elements is the kesterite $Cu_2ZnSn(S,Se)_4$. The PCE of the kesterite-based devices has stagnated at a level lower than 13% [2–4] in the last few years, which is much lower than the predicted value from the Shockley-Queisser limit. This difference between CIGSe and kesterite-based solar cell devices has also motivated research on the other quaternary copper chalcogenide compounds with suitable band gap energy for solar cell absorber. Among them the $Cu_2CdGeSe_4$ compound is less studied, although it has *p*-type conductivity and the band gap energy about 1.20–1.29 eV [5].

There have been number of reports on the synthesis of the $Cu_2CdGeSe_4$ compound by various methods like the horizontal gradient freezing method [6,7]; directional solidification method [8]; Bridgman method [9,10] and solid-state reaction method in sealed evacuated quartz ampoules [5,11,12].

$Cu_2CdGeSe_4$ exists in two modifications of crystal structure such as a tetragonal structure with an *I*-42 m space group and an orthorhombic structure with a $Pmn2_1$ space group [5]. According to [5], the tetragonal structure appears at temperatures lower than 400 °C and/or cooling the samples after synthesis very slowly (~5–10 °C/h) to room temperature (RT). In the earlier studies [13], the optical band gap for tetragonal (*t*-$Cu_2CdGeSe_4$) was found to be 1.29 eV, but later in the study [9], there was experimentally shown that band gap of $Cu_2CdGeSe_4$ at RT is 1.20 eV. Orthorhombic structure (*o*-$Cu_2CdGeSe_4$) has been obtained by cooling the material from 900 °C to 400 °C followed by quenching in cold water [5,11]. The optical absorption measurements showed the band gap of synthesized *o*-$Cu_2CdGeSe_4$ compound ~1.2 eV [6].

The transformation from tetragonal to orthorhombic structure in $Cu_2CdGeSe_4$ was studied in [5]. It was shown that the transformation proceeded slowly and metastable modifications could be persistent for a long time. The *t*-$Cu_2CdGeSe_4$ modification with a tetragonal unit cell has the lattice parameters $a = b = 0.57482(2)$ nm and $c = 1.10533(3)$ nm. The *o*-$Cu_2CdGeSe_4$ modification has lattice parameters $a = 0.80968(9)$, $b = 0.68929(6)$ and $c = 0.66264(6)$ nm [5].

So, there have been made several studies about preparation of two polymorphous modifications of the $Cu_2CdGeSe_4$ compound, but the transformation temperature is not exactly determined and different band gap values have been reported, also these materials have not been

* Corresponding author.
E-mail address: marit.kauk-kuusik@ttu.ee (M. Kauk-Kuusik).

https://doi.org/10.1016/j.tsf.2018.09.025
Received 13 June 2018; Received in revised form 16 August 2018; Accepted 12 September 2018
Available online 13 September 2018
0040-6090/

used as absorber materials in solar cells.

The aim of this study was to synthesize $Cu_2CdGeSe_4$ with two different crystal structure modifications in the monograin powder form in the liquid phase of molten salts and apply these powders as absorber materials in monograin layer (MGL) solar cells.

2. Experimental

In this study $Cu_2CdGeSe_4$ powder materials were synthesized from commercially available CdSe, self-synthesized CuSe, elemental Ge powder and Se shots in the liquid phase of flux materials in evacuated quartz ampoules. Two different salts – cadmium iodide (CdI_2) and potassium iodide (KI) - were used as fluxes. A major technological advantage of the usage of these salts as flux materials is the possibility to remove them after the growth process very easily by a simple dissolution process in water. An additional advantage of the usage of CdI_2 is the low melting temperature of it (T_{melt} = 387 °C [14]) that allows to synthesize of $Cu_2CdGeSe_4$ monograin powders in CdI_2 flux at lower temperatures. In the present study we performed synthesis-growth process in CdI_2 at 500, 600 and 700 °C for 120 h. As the melting temperature of KI is T_{melt} = 681 °C [14], the synthesis-growth of $Cu_2CdGeSe_4$ monograin powders in KI flux was performed at 700 °C, varying synthesis time- 60 and 120 h.

The precursors for synthesis of $Cu_2CdGeSe_4$ were weighted in the molar ratio of elements 2:1:1:4, after that the used flux salt was added with the mass ratio of $m_{precursors}/m_{flux}$ = 1:1. The mixture was degassed and sealed into quartz ampoules and heated at different synthesis temperatures. After cooling down and opening the ampoules the salt was removed from solid powder particles by leaching with deionized H_2O. Then, the powder was dried in thermostat at 50 °C and sieved into narrow size fractions by sieving system Retsch AS 200.

The morphology of synthesized powder crystals was studied by high-resolution scanning electron microscope (HR-SEM Zeiss Merlin). The bulk composition of the synthesized powder crystals was analyzed by energy dispersive X-ray spectroscopy (EDX) on HR-SEM Zeiss Merlin equipped with Bruker EDX-XFlash6/30 detector with an accelerating voltage of 20 kV. Compositional analysis was made from polished individual crystals.

The crystalline structure was studied by X-ray diffraction (XRD) with a Rigaku Ultima IV diffractometer with monochromatic Cu Kα radiation λ = 1.54056 Å at 40 kV and 40 mA, using a D/teX Ultra silicon strip detector.

$Cu_2CdGeSe_4$ powders were also analyzed by RT micro-Raman spectroscopy using Horiba's LabRam HR 800 spectrometer equipped with a multichannel CCD detection system in the backscattering configuration using a 532 nm laser line with a spot size of 5 μm.

As the MGL technology [15] requires powder grains of nearly equal size, the sieve analysis was used to determine the particle size distribution. The particle size distribution helps to determine the suitable growth conditions for the synthesis process of $Cu_2CdGeSe_4$ monograin powders in different fluxes. The most valuable fractions for making MGL's manually in the lab conditions are between 45 and 112 μm. Sieve analysis is used to divide the particulate material into size fractions and then to determine the weight of these fractions. In this way a relatively broad particle size spectrum can be analyzed quickly and reliably. $Cu_2CdGeSe_4$ powders were implemented as absorber materials in MGL solar cells, the scheme of device is shown in Fig. 1. $Cu_2CdGeSe_4$ powder crystals were covered by CdS buffer layer (~45 nm) deposited by the chemical bath deposition method to form the heterojunction and embedded into a thin epoxy layer. *i*-ZnO and conductive ZnO:Al layers were deposited by RF sputtering. The formed structure was glued onto a glass plate. Conductive graphite paste was used to make back contacts and Ag-paste was used to make front collector.

Device current–voltage (*J–V*) characteristics were measured under AM 1.5G (100 mW/cm^2) using a Newport Class AAA solar simulator system. *J–V* characteristics were recorded by a Keithley 2400 source meter. A typical solar cell had an active area of approximately 4 mm^2. External quantum efficiency (EQE) was measured in the spectral region of 350–1235 nm using a computer controlled SPM-2 prism monochromator. The generated photocurrent was detected at 0 V bias voltage at room temperature, a 250 W standard halogen lamp was used as a light source.

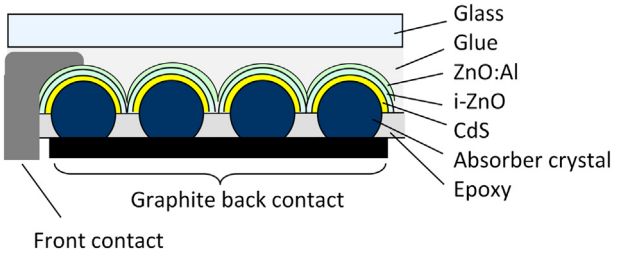

Fig. 1. Scheme of monograin layer solar cell.

3. Results and discussion

3.1. Morphology and particle size distribution

In the molten salt synthesis, a large amount (typically almost equal to the precursor's weight of precursors) of a flux salt is used to provide liquid medium between solid particles that conduces to recrystallization and avoids sintering of solid particles. This liquid phase as solvent controls the characteristics (size, shape, etc.) of the forming powder crystals. Molten medium enhances the rate of solid-state reactions. During the heating up of the mixture of CuSe-Ge-Se-CdSe-CdI_2 to the synthesis-growth temperature, the firstly formed liquid phase is elemental Se (T_{melt} = 221 °C [14]). It means that liquid Se can act as a flux at this temperature, but the volume of this flux is not enough to repel separate solid particles from each other and they start to sinter together. This sintering process arises in heating material below the melting point of the main flux material CdI_2 and continues until CdI_2 melts at 387 °C. Then the volume of the liquid phase exceeds the volume of voids between precursor particles and repelling forces [16] between solid particles arise. In this case, the formed liquid phase is sufficient to repel both, the solid precursor particles and the formed $Cu_2CdGeSe_4$ particles from each other and to avoid sintering caused by the contracting capillary forces arising in the solid–liquid phase boundaries. The sintered together particles are seen in Fig. 2a and Fig. 2b. The sharp edges of the crystals synthesized at 500 °C and 600 °C indicate to the crystal formation mechanism by sintering process and to insufficient recrystallization of crystals in conditions of low solubility of $Cu_2CdGeSe_4$ in CdI_2.

The growth of crystals by Ostwald ripening is characterized by a normal (Gaussian) distribution of grain sizes (see Fig. 3a). The transport of material occurs from smaller to larger grains because of the difference in surface energy and in solubility between the grains of different size. Therefore, small grains dissolve, large grains grow and average grain size increases. High solubility of synthesized material in flux results in spherical grains as seen in Fig. 2c. Rounded grains are synthesized at 700 °C irrespective of the used flux material due to the higher solubility at higher temperatures.

Fig. 3b shows the lognormal plot of the accumulative weight percentage of the particles under a specific particle size versus the particle size for the powder samples synthesized at different temperatures in CdI_2 flux and powders grown in KI flux for different times at 700 °C. The black solid horizontal line marking 50% shows the powder median grain size values (D_{50}) calculated from weight percentage. The D_{50} is the size in micrometers that splits the distribution in half above and half below this diameter. The sieving analysis revealed that median particle size of produced powder crystals increased with increasing synthesis temperature and duration. By increasing the synthesis temperature

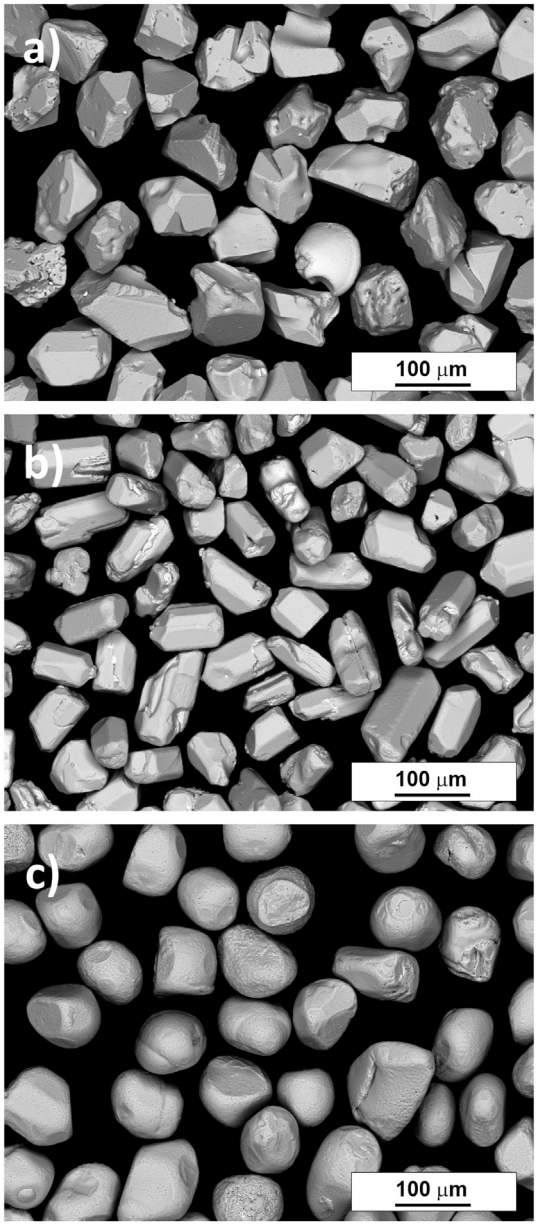

Fig. 2. SEM images of $Cu_2CdGeSe_4$ powder crystals (fraction size 63–75 μm) synthesized at a) 500 °C; b) 600 °C and c) 700 °C for 120 h in the CdI_2 flux.

from 500 to 700 °C the median size of particles grown in CdI_2 increases from 25 to 139 μm. Median size of particles for powders synthesized in KI flux at 700 °C increased from 112 to 132 μm by increasing the

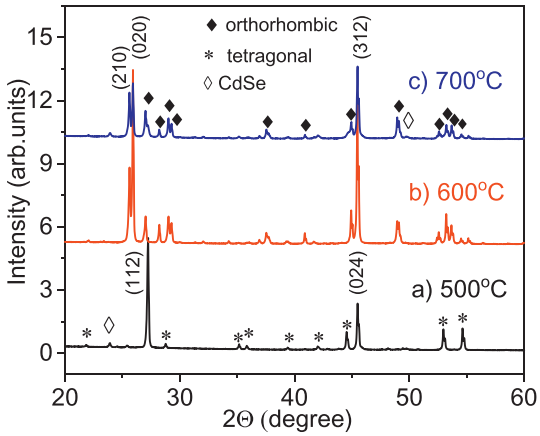

Fig. 4. XRD patterns of $Cu_2CdGeSe_4$ powder synthesized at a) 500 °C; b) 600 °C and c) 700 °C in CdI_2 flux.

Table 1
Lattice parameters of $Cu_2CdGeSe_4$ powders.

Samples	Space group	*a*, Å	*b*, Å	*c*, Å
Powder 1 (500 °C)	*I-42 m*- tetragonal	5.7476	5.7476	11.0511
Powder 2 (600 °C)	*Pmn21*-orthorhombic	8.0726	6.8855	6.6118
Powder 3 (700 °C)	*Pmn21*- orthorhombic	8.0634	6.8793	6.6035

synthesis time from 60 to 120 h. Results show that the median size of particles grown at 700 °C does not depend much on the flux material. The most applicable fractions of crystals for monograin membrane preparation in lab conditions are between 45 and 112 μm, the highest yield in this range was gained by synthesizing the $Cu_2CdGeSe_4$ monograin powder in CdI_2 flux at 600 °C for 120 h.

3.2. Composition

Bulk composition of the $Cu_2CdGeSe_4$ powders synthesized in CdI_2 flux at different temperatures was characterized by EDX. The atomic concentrations of Cu and Se remained almost the same with increasing synthesis temperature, while the atomic concentrations of Cd increased and that of the Ge decreased probably by the reason that CdI_2 is not inactive in the synthesis [18]. By increasing the synthesis temperature from 500 °C to 700 °C, the bulk composition became Cd-rich (the ratio of [Cu]/[Cd] + [Ge]) increases from 0.99 to 1.07). The ratio of [Cu]/([Cd] + [Ge])~1.0 for $Cu_2CdGeSe_4$ powders synthesized in CdI_2 at 500 °C and 700 °C, but powders synthesized at 600 °C have Cu-poor (the ratio of [Cu]/([Cd] + [Ge]) = 0.93) composition probably due to the shape of single phase area of the phase diagram [12]. Bulk composition of the $Cu_2CdGeSe_4$ powders synthesized in KI flux for different times

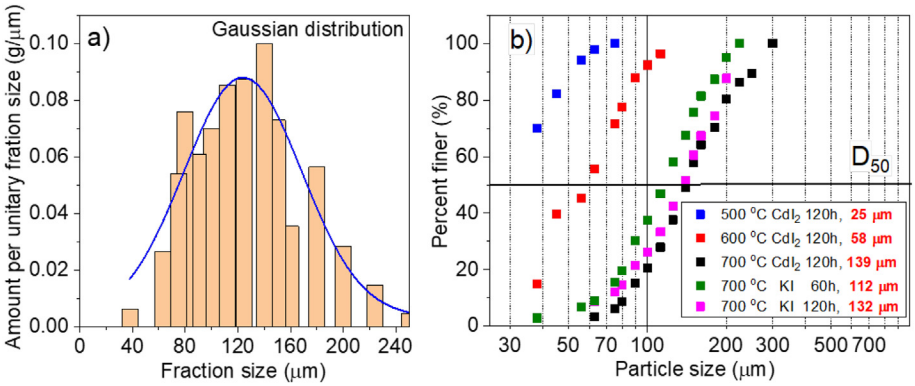

Fig. 3. a) A normal distribution of grain sizes for powder synthesized in KI at 700 °C for 120 h; b) Particle size distribution curves for powders synthesized in CdI_2 and KI at different temperatures for different times. D_{50} marks the median size of particles – written in red (at the peak of Gaussian distribution). (For interpretation of the references to colour in this figure legend, the reader is referred to the web version of this article.)

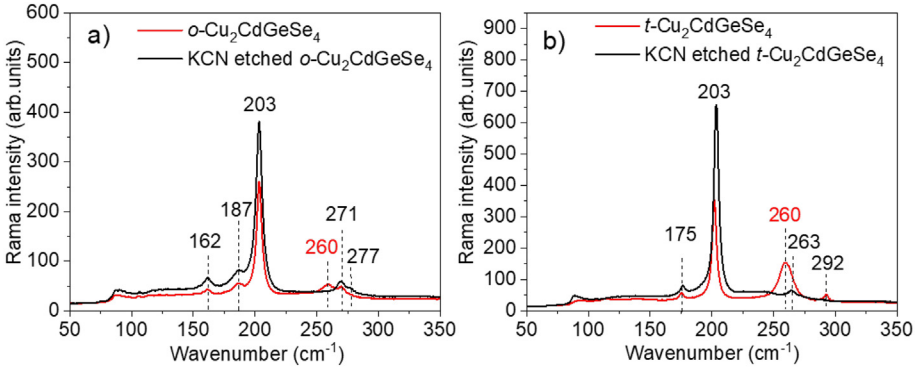

Fig. 5. RT-Raman spectra of $Cu_2CdGeSe_4$ before and after KCN etching - a) with orthorhombic structure and b) with tetragonal structure.

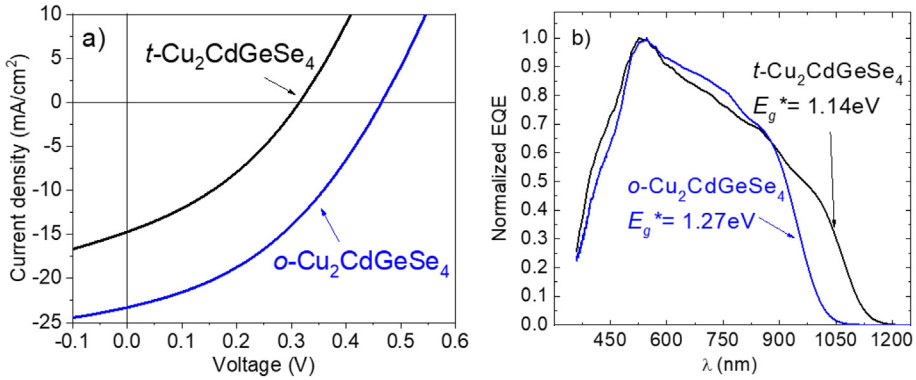

Fig. 6. a) *J-V* characteristics and b) EQE spectra of MGL solar cell prepared from *t*-$Cu_2CdGeSe_4$ and *o*-$Cu_2CdGeSe_4$ powders.

was also Cd-rich (the ratio of [Cd]/[Ge] = 1.03) and did not depend on synthesis time. But the ratio of [Cu]/([Cd] + [Ge]) decreased from 1.0 to 0.96 by increasing the synthesis time.

3.3. XRD analysis

The $Cu_2CdGeSe_4$ powders synthesized in CdI_2 flux at different temperatures were investigated by XRD as shown in Fig. 4. The XRD pattern of the powder synthesized at 500 °C showed peaks corresponding to the tetragonal crystal structure (01-070-9042) with the space group *I-42 m* of the main phase and the presence of CdSe secondary phase. The main peak is attributed to (112) plane of $Cu_2CdGeSe_4$. The powders synthesized at 600 °C and 700 °C revealed the presence of the orthorhombic phase (01–074-3115). Calculated lattice parameters *a*, *b*, *c* of all the samples are presented in the Table 1.

3.4. Raman analysis

Raman spectroscopy was used to analyze the phase composition of all the synthesized $Cu_2CdGeSe_4$ monograin batches. Unfortunately there is no Raman data published for this compound in the literature. The most intensive peak in the spectra of $Cu_2CdGeSe_4$ is observed at 203 cm^{-1} and it is not depending on the phase structure. The additional characteristic Raman modes for the *o*-$Cu_2CdGeSe_4$ phase were detected at 162, 187, 271 and 277 cm^{-1} (see Fig. 5a) and for *t*-$Cu_2CdGeSe_4$ phase, the characteristic peaks were at 175, 263 and 292 cm^{-1} (Fig. 5b).

All the as-grown powders had an additional peak in Raman spectra at 260 cm^{-1}, which has been assigned to $Cu_{2-x}Se$ phase [20]. In order to remove selectively the $Cu_{2-x}Se$ phase from the surface of as-grown $Cu_2CdGeSe_4$ powders, chemical etching with 10% KCN + 1% KOH solution for 30 min was performed. The $Cu_{2-x}Se$ Raman scattering peak at 260 cm^{-1} disappeared completely after the KCN etching while no change was observed in the $Cu_2CdGeSe_4$ peaks.

3.5. MGL solar cell device properties

Sieving analysis showed that the yield of the applicable size of the crystals synthesized at 500 °C for monograin layer solar cell preparation was very small. So, to produce MGL solar cells, the powder synthesized at 700 °C in KI flux was used for the different post-annealing procedures providing the both possible structural modifications of $Cu_2CdGeSe_4$ as solar cell absorber materials. In order to produce *o*-$Cu_2CdGeSe_4$, the powder was post-annealed at 500 °C for 1 h and cooled by quenching into water. *t*-$Cu_2CdGeSe_4$ modification was obtained by applying the same annealing conditions at 500 °C for 1 h, but powder was cooled slowly to room temperature (~0.5 °C/min). XRD patterns of these powders confirmed the formation of different respective modifications.

To investigate the effect of the crystalline structure of $Cu_2CdGeSe_4$ on device performance, *J–V* curves of the solar cell devices were measured under AM1.5 illumination, as shown in Fig. 6a. For the device based on *t*-$Cu_2CdGeSe_4$ absorber, the highest obtained power conversion efficiency (PCE) was 2.16% with V_{oc} of 315 mV, J_{sc} of 14.7 mA/cm^2, and *FF* of 35%, while for the *o*-$Cu_2CdGeSe_4$ solar cell, a PCE of 4.21% was achieved, with a V_{oc} of 464 mV, J_{sc} of 17.5 mA/cm^2 and *FF* of 39%. These initial results indicate that both - *t*-$Cu_2CdGeSe_4$ and *o*-$Cu_2CdGeSe_4$ materials are potential candidates for absorber material in photovoltaic devices. However, more information on the dependence of the optoelectronic properties as well as the structural properties on the composition and material preparation conditions is needed in order to optimize the technology.

EQE analysis was used to estimate the effective bandgap energy (E_g*) of the synthesized absorber materials [21] since the evaluation of E_g from the optical absorption or reflectance spectra of the monograins is rather challenging. The EQE of $Cu_2CdGeSe_4$ solar cells was measured as a function of the wavelength of the incident light at room

temperature (see Fig. 6b). From the linear segment of the low-energy side of the construction $(E^*QE)^2$ vs. E curves, the E_g^* can be evaluated. The E_g^* values obtained from EQE measurements was found to be 1.27 eV for orthorhombic $Cu_2CdGeSe_4$ powders and 1.14 eV for tetragonal $Cu_2CdGeSe_4$ powders.

4. Conclusions

$Cu_2CdGeSe_4$ powders for photovoltaic applications were synthesized by molten salt method in CdI_2 and KI. Phase analysis by Raman spectroscopy and X-ray diffraction showed that $Cu_2CdGeSe_4$ powder synthesized at 500 °C had tetragonal structure and powders synthesized at temperatures 600 °C and 700 °C had orthorhombic structure regardless of the used molten salt. The results of compositional analysis indicated that Cu-poor and Cd-rich powders were synthesized in KI flux at 700 °C and in CdI_2 flux at 600 °C. The band gap values determined from EQE measurements were found to be 1.27 eV for orthorhombic $Cu_2CdGeSe_4$ and 1.14 eV for tetragonal $Cu_2CdGeSe_4$ material. The best PCE of 4.21% was achieved by using the orthorhombic structured $Cu_2CdGeSe_4$ powder as absorber material.

Acknowledgements

The authors acknowledge Dr. A. Mere for recording the XRD patterns. This work was supported by the Estonian Research Council under the contract IUT19-28 and the Estonian Centre of Excellence in Research project “Advanced materials and high-technology devices for sustainable energetics, sensorics and nanoelectronics“(TK141).

References

[1] Solar Frontier press release dated, http://www.solar-frontier.com/eng/news/2017/1220_press.html, (December 8, 2017).
[2] W. Wang, M.T. Winkler, O. Gunawan, T. Gokmen, T.K. Todorov, Y. Zhu, D.B. Mitzi, Device Characteristics of CZTSSe Thin-Film Solar Cells with 12.6% Efficiency, Adv. Energy Mater. 4 (2014) 1301465, , https://doi.org/10.1002/aenm.201301465.
[3] T. Taskesen, J. Neerken, J. Schoneberg, D. Pareek, V. Steininger, J. Parisi, L. Gütay, Adv. Energy Mater. 8 (16) (2018) 1703295, , https://doi.org/10.1002/aenm.201703295.
[4] Y.S. Lee, T. Gershon, O. Gunawan, T.K. Todorov, T. Gokmen, Y. Virgus, S. Guha, $Cu_2ZnSnSe_4$ Thin-Film Solar Cells by thermal Co-evaporation with 11.6% Efficiency and improved Minority carrier Diffusion Length, Adv. Energy Mater. 5 (2015) 1401372, , https://doi.org/10.1002/aenm.201401372.
[5] L.D. Gulay, Ya.E. Romanyuk, O.V. Parasyuk, Crystal structures of low- and high-temperature modifications of $Cu_2CdGeSe_4$, J. Alloys Compd. 347 (2002) 193–197, https://doi.org/10.1016/S0925-8388(02)00790-9.
[6] H. Matsushita, T. Maeda, A. Katsui, T. Takizawa, Thermal analysis and synthesis from the melts of Cu-based quaternary compounds Cu–III–IV–VI_4 and Cu_2–II–IV–VI_4 (II = Zn, Cd; III = Ga, In; IV = Ge, Sn; VI = Se), J. Cryst. Growth 208 (2000) 416–422, https://doi.org/10.1016/S0022-0248(99)00468-6.
[7] H. Matsushita, T. Ichikawa, A. Katsui, Structural, thermodynamical and optical properties of Cu_2-II-IV-VI_4 quaternary compounds, J. Mater. Sci. 40 (2005) 2003–2005, https://doi.org/10.1007/s10853-005-1223-5.
[8] N.N. Konstantinova, G.A. Medvedkin, I.K. Polushina, Yu.V. Rud, A.D. Smirnova, V.I. Sokolova, M.A. Tairov, Optical and electric properties of $Cu_2CdSnSe_4$ and $Cu_2CdGeSe_4$, Izv. Akad. Nauk SSSR Neorgan. Mater. (rus) 25 (1989) 1445–1448.
[9] M.G. Brik, O.V. Parasyuk, G.L. Myronchuk, I.V. Kityk, Specific features of band structure and optical anisotropy of $Cu_2CdGeSe_4$ quaternary compounds, Mater. Chem. Phys. 147 (2014) 155–161, https://doi.org/10.1016/j.matchemphys.2014.04.022.
[10] V.A. Ocheretova, O.V. Parasyuk, A.O. Fedorchuk, O.Y. Khyzhun, Electronic structure of $Cu_2CdGeSe_4$ single crystal as determined from X-ray spectroscopy data, Mater. Chem. Phys. 160 (2015) 345–351, https://doi.org/10.1016/j.matchemphys.2015.04.049.
[11] R. Chetty, J. Dadda, J. de Boor, E. Müller, R.C. Mallik, The effect of Cu addition on the thermoelectric properties of $Cu_2CdGeSe_4$, Intermetallics 57 (2015) 156–162, https://doi.org/10.1016/j.intermet.2014.10.015.
[12] L.V. Piskach, O.V. Parasyuk, Ya.E. Romanyuk, The phase equilibria in the quasi-binary Cu_2GeS_3/Se_3/–CdS/Se/ systems, J. Alloys Compd. 299 (2000) 227–231, https://doi.org/10.1016/S0925-8388(99)00797-5.
[13] S.A. Mkrtchyan, K. Dovletov, E.G. Zhukov, A.G. Melikdzhanyan, S. Nuryev, Electrical properties of $Cu_2A^2B^4Se_4$ compounds (A^2-Cd, Hg; B^4-Ge, Sn), Izv. Akad. Nauk SSSR Neorgan. Mater. (rus) 24 (7) (1988) 1094–1096.
[14] CRC Handbook of Chemistry and Physics 84th Edition by David R. Lide, CRC Press LLC (2003).
[15] E. Mellikov, M. Altosaar, M. Kauk-Kuusik, K. Timmo, D. Meissner, M. Grossberg, J. Krustok, O. Volobujeva, Growth of CZTS-based monograins and their application to membrane solar cells, in: K. Ito (Ed.), Copper Zinc Tin Sulfide-Based Thin-Film Solar Cells, John Wiley & Sons Ltd, 2015, pp. 289–309, , https://doi.org/10.1002/9781118437865.ch13.
[16] Suk-Joong L. Kang, Sintering, Densification, Grain Growth, and Microstructure, Elsevier Ltd, 2015, https://doi.org/10.1016/B978-0-7506-6385-4.X5000-6.
[18] I. Leinemann, G.C. Nkwusi, K. Timmo, O. Volobujeva, M. Danilson, J. Raudoja, T. Kaljuvee, R. Traksmaa, M. Altosaar, D. Meissner, Reaction pathway to $Cu_2ZnSnSe_4$ formation in CdI_2, Part 1. Chemical reactions and enthalpies in mixtures of CdI_2-ZnSe, CdI_2-SnSe, and CdI_2-CuSe, J. Therm. Anal. Calorim. (2018) 1–13, https://doi.org/10.1007/s10973-018-7102-5.
[20] T. Tanaka, T. Sueishi, K. Saito, Q. Guo, M. Nishio, K.M. Yu, W. Walukiewicz, Existence and removal of Cu_2Se second phase in coevaporated $Cu_2ZnSnSe_4$ thin films, J. Appl. Phys. 111 (2012) 053522, , https://doi.org/10.1063/1.3691964.
[21] J. Krustok, R. Josepson, T. Raadik, M. Danilson, Potential fluctuations in $Cu_2ZnSnSe_4$ solar cells studied by temperature dependence of quantum efficiency curves, Physica B 405 (15) (2010) 3186–3189, https://doi.org/10.1016/j.physb.2010.04.041.